ChemComm

Accepted Manuscript

This article can be cited before page numbers have been issued, to do this please use: K. Cai, Y. Tan, C. Tan, J. Wu, P. Wu, J. Liang, S. Liu, B. Zhang and Y. Jiang, *Chem. Commun.*, 2017, DOI: 10.1039/C7CC00850C.

ROYAL SOCIETY OF CHEMISTRY

rsc.li/chemcomm

Journal Name

View Article Online
DOI: 10.1039/C7CC00850C

COMMUNICATION

Iminodiacetate-modified conjugated polyelectrolyte for fluorescent labeling of histidine-tagged proteins

Received 00th January 20xx,
Accepted 00th January 20xx

DOI: 10.1039/x0xx00000x

www.rsc.org/

Kai Cai,[†ab] Ying Tan,[†ab] Chunyan Tan,*[ab] Jiatao Wu,[ab] Pan Wu,[ab] Jiamei Liang,[ab] Shuwen Liu,[ab] Bibo Zhang,[ab] and Yuyang Jiang[bc]

The iminodiacetate-Ni^{2+}-hexahistidine system is extensively used in protein purification. In this study, an anionic conjugated polyelectrolyte (CPE) with a poly(p-pheynylene ethynylene) backbone and iminodiacetate side chains, named PPEIDA, was designed and synthesized. Recognition and visualization of hexahistidine-tagged (His-tagged) proteins using PPEIDA was demonstrated.

Conjugated polyelectrolytes (CPEs), which consist of electron-delocalized conjugated backbones with charged side groups, have been extensively studied due to their strong light absorption, high fluorescence quantum yields, and signal amplification properties.[1-5] Many commonly used charged side moieties, such as carboxylate, sulfonate, phosphate, alkyl ammonium groups, etc., have been reported to enhance the water-solubility and biocompatibility of CPEs.[4, 6-10] Over the past decades, the introduction of pendant charged groups enable CPEs to interact with species with opposite charges through electrostatic attractions, enhancing their applicability as potential fluorescent chemosensors and biosensors as well as fluorescent cell imaging materials.[1-5, 11-13] However, non-specific electrostatic interactions have been reported as perturbations, sacrificing the sensitivity and selectivity of CPEs in recognition of targets.[14, 15] Therefore, there is a significant challenge and demand to develop novel CPEs with specific target recognition elements in order to practically use CPEs in biological studies. Some CPEs grafting with folic acid,[16-18] lipid,[19] antibodies,[20, 21] and peptides[22] have been reported to recognize specific receptors or proteins. For example, folate-substituted poly(p-phenyleneethynylene) (PPE) was efficiently used in cancer cell imaging due to the specific interaction between folate and folate-receptors overexpressed in some tumor cells.[16-18]

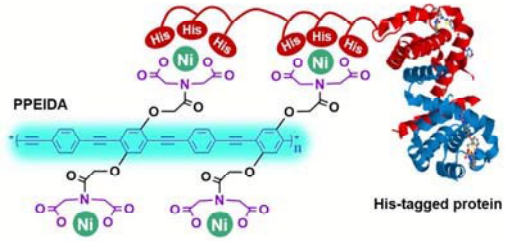

Scheme 1 Schematic illustration of PPEIDA-Ni^{2+} complex coupled to His-tagged protein.

Iminodiacetate (IDA) and nitrilotriacetate (NTA) are commonly known as complexes with Ni^{2+}, which consequently bind to the hexahistidine tag (His-tag).[23, 24] Thus, IDA-Ni^{2+}-His-tag and NTA-Ni^{2+}-His-tag systems have been seen in small molecular probes as well as surface-modified nanoparticles to immobilize and purify recombinant proteins in biological studies.[25-34] CPEs have emerged as a new material platform in biological studies and applications due to their strong fluorescence, good bio-compatibility, low cytotoxicity, and excellent photostability. Herein, we report a novel CPE with IDA side chains pendant on a PPE backbone, named as PPEIDA, which can be used for the recognition of His-tagged proteins through fluorescence anisotropy (FA) and Förster resonance energy transfer (FRET). The proposed PPEIDA-Ni^{2+} complex could find its potential applications in the development of an alternative to the conventional Western blotting method, as well as specific cell imaging.

PPEIDA was synthesized via Sonogashira protocol.[35] Generally speaking, the ester precursor PPE-iminodiacetate ester was synthesized first with the two building blocks of iminodiacetic ester-substituted diiodobenzene and 1,4-diethynylbenzene using $Pd(PPh_3)_4$ and CuI as catalysts. The following hydrolysis of the ester polymer gave the final polymer, PPEIDA (Scheme S1, ESI†). The molecular weight (MW) of PPEIDA was determined by Maldi-Tof mass spectrometry. The number average MW $\overline{Mn}$, value was 22.5 kD, while the weight average MW $\overline{Mw}$, was 45.6 kD, corresponding to the polydispersity index (PDI) at 2.04. As shown in the structure in Scheme 1, IDA groups on the polymer side chains contributed two chelating ligands to each repeating unit and were proposed to coordinate with metal

[a] Department of Chemistry, Tsinghua University, Beijing 100084, P. R. China.
[b] The State Key Laboratory Breeding Base-Shenzhen Key Laboratory of Chemical Biology, the Graduate School at Shenzhen, Tsinghua University, Shenzhen 518055, P. R. China. Email: tancy@sz.tsinghua.edu.cn; Tel: 86-755-26036533.
[c] School of Pharmaceutical Sciences, Tsinghua University, Beijing 100084, P. R. China.
†These authors contributed equally to this work. Electronic Supplementary Information (ESI) available: Experimental including materials, synthesis, instrumentation and some supplementary figures. See DOI:10.1039/x0xx00000x

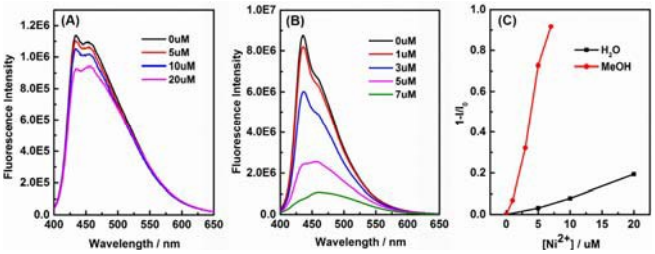

Fig. 1 Fluorescence emission quenching spectra of 1.125 μM PPEIDA with different concentrations of Ni^{2+} in (A) H_2O and (B) MeOH. (C) Quenching efficiency of PPEIDA. I_0 and I are the fluorescence intensities of PPEIDA in the absence and presence of Ni^{2+}, respectively.

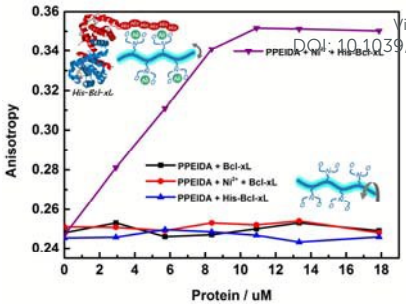

Fig. 2 Fluorescence anisotropy of PPEIDA in response to varying concentrations of Bcl-xL or His-tagged Bcl-xL in the presence or absence of Ni^{2+}; schematic diagram of fluorescence anisotropy variation.

ions, such as Ni^{2+}. Thus, protein recognition was achieved by the multivalent chelation between Ni^{2+} and His-tagged proteins. The UV-Vis absorption and fluorescence emission spectra of PPEIDA showed typical characteristics of PPE polymers with broad absorption from 350 to 450 nm and emission from 400 to 600 nm (Fig. S1, ESI†).

Numerous studies have shown that fluorescence quenching of CPEs could be induced by either electron transfer or energy transfer mechanism.[36-38] In addition, CPE aggregation also causes fluorescence emission to decrease.[6, 39, 40] Fluorescence properties of PPEIDA under the effect of different metal ions, including Ni^{2+}, Zn^{2+}, Mg^{2+}, and Ca^{2+}, in methanol and aqueous solutions were characterized. As shown in Fig. 1, the fluorescence emission of PPEIDA decreased more efficiently by adding Ni^{2+} in methanol compared to that in aqueous solution. There was almost 83.6% quenching by Ni^{2+} at the concentration of 7 μM in methanol solution, while only about 13.5% quenching of PPEIDA by Ni^{2+} at the concentration of 20 μM in aqueous solution. Several other metal ions, including Zn^{2+}, Mg^{2+}, and Ca^{2+}, also showed stronger quenching in methanol than in aqueous solution (Fig. S2, ESI†). These interesting results might be due to polymer aggregation induced by the complexation of the IDA ligand with metal ions in methanol solution. Due to the strong interaction between PPEIDA and Ni^{2+}, this system was further explored for His-tagged proteins recognition using different spectroscopic strategies.

As an important spectroscopic tool, fluorescence anisotropy (FA) is widely used in study of molecular interactions, especially in biological systems.[41, 42] Using this method, protein binding to the fluorescent PPEIDA to form a complex of PPEIDA-Ni^{2+}-His-tagged protein can be detected by the FA signal enhancement resulting from increases in complex volume and/or decreases in PPEIDA flexibility. IDA chelated Ni^{2+} with three valencies, while the other 3 valencies were used for binding His-tagged residues. Fig. 2 shows the principle for FA sensing of the PPEIDA-Ni^{2+} complex with and without the His-tagged protein. As shown in Fig. 2, FA increased from 0.25 to 0.35 in the presence of PPEIDA, Ni^{2+}, and His-tagged Bcl-xL. In the presence of 200 μM Ni^{2+}, the FA signal reached a plateau when the concentration of His-tagged Bcl-xL increased to 11 μM. However, as a distinctive comparison, all three control experiments, including PPEIDA with non-tagged Bcl-xL, PPEIDA with Ni^{2+} and non-tagged Bcl-xL, and PPEIDA with His-tagged Bcl-xL in the absence of Ni^{2+}, did not show any obvious FA signal change. Overall, the addition of Bcl-xL without His-tag, or without Ni^{2+}, had no effect on FA, which highly suggests that Ni^{2+} acts as a bridge ligand for the complexation of PPEIDA-Ni^{2+} with the His-tagged Bcl-xL. As a distinctive comparison, other divalent metal cations, such as Zn^{2+}, Mg^{2+} and Ca^{2+}, didn't bridge the binding between PPEIDA and His-tagged proteins (Figure. S3, ESI†). The plot of anisotropy versus protein concentrations was fitted into a single-site binding model and the binding constant between PPEIDA-Ni^{2+} and the protein was determined to be 1.02×10^6 M^{-1}. Compared to commonly used protein fluorescent labeling techniques, our method provides a feasible and convenient approach to label recombinant His-tagged proteins, without complicated operation in either chemical synthesis or genetically encoding of fluorescent proteins.

FRET is another fluorescent technique commonly used in biological research, which takes place through dipole-dipole coupling when a donor fluorophore and an acceptor have good spectral overlap, parallel transition dipole orientation, and are in close proximity, typically 10-100 Å.[43] Therefore, FRET is a powerful tool, also termed as a "molecular ruler", to measure the distance between two sites comparable to the dimensions of biological macromolecules. FRET experiments were conducted using a recombinant His-tagged red fluorescent protein (RFP). The schematic representation of FRET from PPEIDA to His-tagged RFP is shown in Fig. 3A. RFP absorbs visible light at λ_{max} = 550 nm and emits at λ_{max} = 580 nm. It is weakly fluorescent in water when excited at 380 nm (Fig. S4, ESI†). Due to the good overlap of the fluorescence emission of PPEIDA and the absorption of RFP (Fig. S5, ESI†), it is feasible that the FRET occurs from PPEIDA to RFP, when they

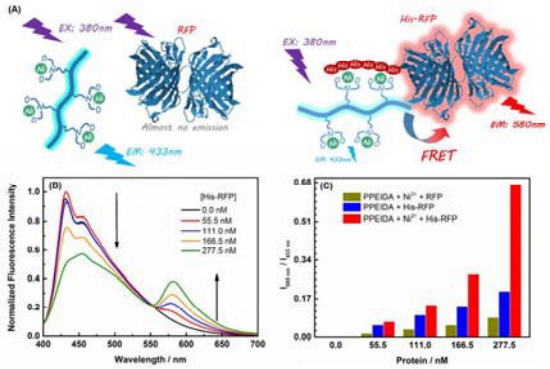

Fig. 3 (A) Schematic representation of FRET from PPEIDA to His-RFP. (B) Normalized fluorescence spectra (λ_{ex} = 380 nm) of PPEIDA-Ni^{2+} complex upon addition of His-RFP (0-277.5 nM) in aqueous solution. Arrows show direction of change of the bands with increasing [His-RFP]. (C) Ratio of intensities at 580 and 433 nm of PPEIDA or PPEIDA-Ni^{2+} complex after addition of RFP or His-RFP, respectively, at various concentrations in aqueous solution.

View Article Online
DOI: 10.1039/C7CC00850C

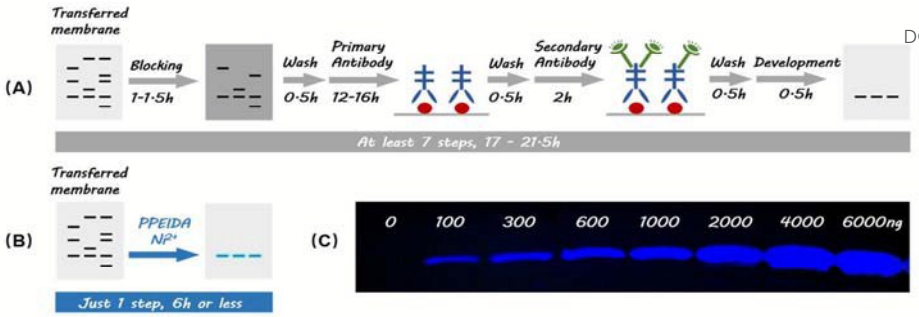

Fig. 4 Procedure comparison of (B) our method to the (A) conventional Western blot analysis. (C) Results of PPEIDA-Ni^{2+} complex-based Western blot analysis for His-tagged protein detection. Protein quantities over a range from 100 to 6000 ng.

are reasonably close to each other. The Förster radius, R_0, between the donor polymer and the acceptor RFP was calculated as 4.83 nm (Table S1, ESI†). Fig. 3B illustrates the changes in fluorescence that occurred concomitant with addition of His-tagged RFP to an aqueous buffer solution of PPEIDA with the presence of Ni^{2+}. The fluorescence of PPEIDA at 433 nm was quenched, while a new emission band emerged at 580 nm from His-RFP. Importantly, under the same excitation conditions, the fluorescence from His-tagged RFP alone is negligible (Fig. S4, ESI†), which confirms the occurrence of the FRET process.

The FRET efficiency is evaluated by the ratio of the fluorescence intensity at 580 and 433 nm (Fig. 3C). Three systems were compared, including PPEIDA-Ni^{2+}-RFP (non His-tagged), PPEIDA-His-tagged RFP (without Ni^{2+}) and PPEIDA-Ni^{2+}-His-tagged RFP. PPEIDA-Ni^{2+}-His-tagged RFP system appeared to have the most responsive FRET, which increased to 0.67 as the protein concentration increased from 0 to 7.5 μg/mL. In the absence of Ni^{2+}, I580/I433 of PPEIDA-His-tagged RFP complex still showed a certain increase (Fig. S6A, ESI†) up to 0.20, which is likely due to the electrostatic attraction between the positively charged histidine residues and negatively charged iminodiacetates that brings His-tagged RFP and PPEIDA closer. The calculated donor-acceptor distances are 4.76 nm and 10.39 nm, for PPEIDA-Ni^{2+}-His-tagged RFP and PPEIDA-His-tagged RFP, respectively, when [His-tagged RFP] = 277.5 nM (Table S1, ESI†). These results suggest that Ni^{2+} can bring the polymer and the protein to a closer proximity for an efficient FRET in the case of PPEIDA-Ni^{2+}-His-RFP. When RFP has no His-tag, I580/I433 showed minimum increase during the addition of protein (Fig. S6B, ESI†). When either Ni^{2+} was replaced by other metal ions, including Zn^{2+}, Mg^{2+}, and Ca^{2+}, or no metal ions was present, no obvious FRET was observed, indicating that Ni^{2+} played an important role in connecting the polymer probe and the target protein (Fig. S7, ESI†).

Both FA and FRET studies encouraged us to further explore the possibility of using this novel PPEIDA-Ni^{2+}-His-tagged protein system in fluorescent labeling applications. Western blot analysis is a widely used analytical technique in molecular biology to detect and quantify specific proteins in a homogenate or extracted sample from tissue or cells. The main principle behind Western blot analysis is to utilize an antigen-antibody immune reaction.[44, 45] However, this technique is time-consuming and laborious. It was expected that using the PPEIDA-Ni^{2+} complex to fluorescently label His-tagged proteins would provide a simple, time-saving, and sensitive method for Western blot analysis. Due to the extensive use of recombinant His-tagged proteins in biological research, a simplified Western blot method would be a valuable alternative for the detection of recombinant proteins. The conventional method requires at least 7 steps and 17~21.5 h to complete the procedure. As shown in Fig. 4, our method (Fig. 4B) dramatically reduced the number of steps, time, and costs compared to those in conventional Western blot analysis (Fig. 4A). To the best of our knowledge, there have been no reports on the direct use of fluorescent CPE-Ni^{2+} complex, which eliminated the laborious primary and secondary antibody binding and wash steps, in a Western blotting application. The time spent on Western blot using our method is even comparable to some automatic Western blot instruments, which cost about 4 hours. Another advantage is that our method provided high-quality and reproducible fluorescent protein bands. As shown in Fig. 4C, fluorescence signals are proportional to protein quantities over a range from 100 to 6000 ng. This method thus provides a quantitative analysis of Western blots more easily and more reliable. Moreover, owing to the extraordinary optical properties of CPEs, our system can harness high brightness and extreme stability, which showed minimal fluorescence decline in blots even after exposure to the air after one year on the shelf.

The MTT assay was utilized to evaluate the cell cytotoxicity of PPEIDA (Fig. S8, ESI†). PPEIDA treated HeLa cells showed cell viability about 95% at the highest concentration of 200 μM. The low cytotoxicity of PPEIDA makes it a good material for vivo cell imaging applications. *In-situ* fluorescent labeling of His-tagged proteins was carried out using PPEIDA-Ni^{2+} on cell membranes under live cell conditions. Bradykinin receptor type2 (B2R) was tethered with a His-tag at the exoplasmic N-terminus and employed as the target protein expressed on cell surfaces. In cell imaging experiments, HeLa cells expressing His-tagged B2R were incubated with PPEIDA-Ni^{2+} PBS solution (3.25 μM PPEIDA, 200 μM Ni^{2+}) for 3 min and then washed by

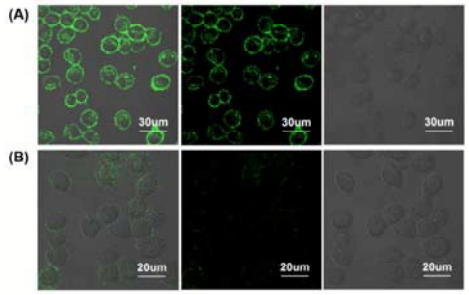

Fig. 5 Visualization of the His-B2R in Hela cells. HeLa cells expressing His-B2R were incubated with (A) PPEIDA-Ni^{2+} PBS solution and (B) PPEIDA PBS solution. Cells were washed before imaging. Scale bar: (A) 30 μm; (B) 20 μm.

imidazole PBS solution (5 mM) to remove unbound PPEIDA-Ni^{2+} complexes. The clear fluorescence on the cell surfaces wasobserved by confocal laser scanning microscopy (CLSM) (Fig. 5A). In contrast, after the same treatment, negligible green fluorescence was observed without the presence of Ni^{2+}, which suggested that Ni^{2+} played a key role in labeling the His-tagged B2R.

In conclusion, we have successfully designed and synthesized an anionic CPE, PPEIDA, with iminodiacetate pendant groups. This polymer forms chelating complex with transition metal ion Ni^{2+}, and thus can be exploited to coordinatively interact with His-tagged proteins. Both FA and FRET experiments demonstrated the prominent recognition of His-proteins using PPEIDA-Ni^{2+} complex. Compared to the conventional Western blot analysis, our method using PPEIDA-Ni^{2+} significantly reduced the operation time and cost. Our proof-of-concept study showed that the minimum protein quantity being successfully detected was 100 ng, which could be further optimized to suite high-sensitivity requirement. Moreover, PPEIDA-Ni^{2+} complex demonstrated specific fluorescent labeling of His-tagged proteins overexpressed on cell membranes under live cell conditions. These results are expected to expand new applications for CPEs in specific protein labeling, for example, imaging proteins of interest in live cells, tracking cellular events, and studying protein-protein-interactions, with minimal functional perturbation.

The authors would like to thank the financial supports from National Natural Science Foundation of China (No. 21572115 and 21302108), and Shenzhen Municipal Government (JCYJ20160301153959476 and JCYJ20160324163734374).

Notes and references

1. T. M. Swager, *Acc. Chem. Res.*, 1998, **31**, 201-207.
2. D. T. McQuade, A. E. Pullen and T. M. Swager, *Chem. Rev.*, 2000, **100**, 2537-2574.
3. S. W. Thomas, G. D. Joly and T. M. Swager, *Chem. Rev.*, 2007, **107**, 1339-1386.
4. H. Jiang, P. Taranekar, J. R. Reynolds and K. S. Schanze, *Angew. Chem. Int. Ed.*, 2009, **48**, 4300-4316.
5. S. b. Rochat and T. M. Swager, *ACS Appl. Mater. Interfaces*, 2013, **5**, 4488-4502.
6. Z. Chen, P. Wu, R. Cong, N. Xu, Y. Tan, C. Tan and Y. Jiang, *ACS Appl. Mater. Interfaces*, 2015, **8**, 3567-3574.
7. Y. Liu, P. Wu, J. Jiang, J. Wu, Y. Chen, Y. Tan, C. Tan and Y. Jiang, *ACS Appl. Mater. Interfaces*, 2016, **8**, 21984-21989.
8. Z. Yao, Y. Li, C. Li and G. Shi, *Chem. Commun.*, 2010, **46**, 8639-8641.
9. Z. Yao, X. Hu, B. Huang, L. Zhang, L. Liu, Y. Zhao and H. Wu, *ACS Appl. Mater. Interfaces*, 2013, **5**, 5783-5787.
10. Z. Yao, Y. Yang, X. Chen, X. Hu, L. Zhang, L. Liu, Y. Zhao and H. Wu, *Anal. Chem.*, 2013, **85**, 5650-5653.
11. Y. Liu, K. Ogawa and K. S. Schanze, *J. Photochem. Photobiol., C*, 2009, **10**, 173-190.
12. X. Feng, L. Liu, S. Wang and D. Zhu, *Chem. Soc. Rev.*, 2010, **39**, 2411-2419.
13. C. Zhu, L. Liu, Q. Yang, F. Lv and S. Wang, *Chem. Rev.*, 2012, **112**, 4687-4735.
14. S. J. Dwight, B. S. Gaylord, J. W. Hong and G. C. Bazan, *J. Am. Chem. Soc.*, 2004, **126**, 16850-16859.
15. O. R. Miranda, C. You, R. Phillips, I. Kim, P. S. Ghosh, U. H. Bunz and V. M. Rotello, *J. Am. Chem. Soc.*, 2007, **129**, 9856-9857.
16. K. Pu, K. Li and B. Liu, *Adv. Funct. Mater.*, 2010, **20**, 2770-2777.
17. C. Xing, L. Liu, H. Tang, X. Feng, Q. Yang, S. Wang and G. C. Bazan, *Adv. Funct. Mater.*, 2011, **21**, 4058-4067.
18. I.-B. Kim, H. Shin, A. J. Garcia and U. H. Bunz, *Bioconjug. Chem.*, 2007, **18**, 815-820.
19. X. Feng, Y. Tang, X. Duan, L. Liu and S. Wang, *J. Mater. Chem.*, 2010, **20**, 1312-1316.
20. K. Pu, J. Shi, L. Cai, K. Li and B. Liu, *Biomacromolecules*, 2011, **12**, 2966-2974.
21. D. G. Colak, I. Cianga, D. O. Demirkol, O. Kozgus, E. I. Medine, S. Sakarya, P. Unak, S. Timur and Y. Yagci, *J. Mater. Chem.*, 2012, **22**, 9293-9300.
22. L. Feng, J. Zhu and Z. Wang, *ACS Appl. Mater. Interfaces*, 2016, **8**, 19364-19370.
23. J. Porath, J. Carlsson, I. Olsson and G. Belfrage, *Nature*, 1975, **258**, 598-599.
24. E. Hochuli, H. Döbeli and A. Schacher, *J. Chromatogr. A*, 1987, **411**, 177-184.
25. C. R. Goldsmith, J. Jaworski, M. Sheng and S. J. Lippard, *J. Am. Chem. Soc.*, 2006, **128**, 418-419.
26. Y. Lai, Y. Chang, L. Hu, Y. Yang, A. Chao, Z. Du, J. A. Tanner, M. Chye, C. Qian and K. Ng, *Proc. Natl. Acad. Sci. U. S. A.*, 2015, **112**, 2948-2953.
27. S. Lata, M. Gavutis, R. Tampé and J. Piehler, *J. Am. Chem. Soc.*, 2006, **128**, 2365-2372.
28. S. Lata, A. Reichel, R. Brock, R. Tampé and J. Piehler, *J. Am. Chem. Soc.*, 2005, **127**, 10205-10215.
29. I. Takahira, H. Fuchida, S. Tabata, N. Shindo, S. Uchinomiya, I. Hamachi and A. Ojida, *Bioorg. Med. Chem. Lett.*, 2014, **24**, 2855-2858.
30. K. M. Harmatys, E. L. Cole and B. D. Smith, *Mol. Pharm.*, 2013, **10**, 4263-4271.
31. M. Bloemen, L. Vanpraet, M. Ceulemans, T. Parac-Vogt, K. Clays, N. Geukens, A. Gils and T. Verbiest, *RSC Adv.*, 2015, **5**, 66549-66553.
32. P. K. Bae, K. N. Kim, S. J. Lee, H. J. Chang, C. K. Lee and J. K. Park, *Biomaterials*, 2009, **30**, 836-842.
33. M. J. Kim, H.-Y. Park, J. Kim, J. Ryu, S. Hong, S.-J. Han and R. Song, *Anal. Biochem.*, 2008, **379**, 124-126.
34. S. Uchinomiya, H. Nonaka, S. Wakayama, A. Ojida and I. Hamachi, *Chem. Commun.*, 2013, **49**, 5022-5024.
35. Y. Wu, Y. Tan, J. Wu, S. Chen, Y. Z. Chen, X. Zhou, Y. Jiang and C. Tan, *ACS Appl. Mater. Interfaces*, 2015, **7**, 6882-6888.
36. Y. Xie, Y. Tan, R. Liu, R. Zhao, C. Tan and Y. Jiang, *ACS Appl. Mater. Interfaces*, 2012, **4**, 3784-3787.
37. Y. Xie, R. Zhao, Y. Tan, X. Zhang, F. Liu, Y. Jiang and C. Tan, *ACS Appl. Mater. Interfaces*, 2011, **4**, 405-410.
38. Q. Zhou and T. M. Swager, *J. Am. Chem. Soc.*, 1995, **117**, 12593-12602.
39. C. Tan, M. R. Pinto and K. S. Schanze, *Chem. Commun.*, 2002, 446-447.
40. C. Tan, E. Atas, J. G. Müller, M. R. Pinto, V. D. Kleiman and K. S. Schanze, *J. Am. Chem. Soc.*, 2004, **126**, 13685-13694.
41. G. Weber, *Biochem. J.*, 1952, **51**, 145.
42. G. Weber, *Biochem. J.*, 1952, **51**, 155.
43. J. R. Lakowicz, *Principles of Fluorescence Spectroscopy*, Springer, Baltimore, MD, USA, 2006.
44. J. Renart, J. Reiser and G. R. Stark, *Proc. Natl. Acad. Sci. U. S. A.*, 1979, **76**, 3116-3120.
45. H. Towbin, T. Staehelin and J. Gordon, *Proc. Natl. Acad. Sci. U. S. A.*, 1979, **76**, 4350-4354.